Electronic Supplementary Material (ESI) for ChemComm.

Electronic Supplementary Information

Water Oxidation behind Photoreduction of Graphene Oxide

Hongjiang Li, Xuedan Song, Yantao Shi, Yan Gao, Duanhui Si, Ce Hao**

State Key Laboratory of Fine Chemicals, School of Chemistry, Dalian University of Technology, Dalian, 116024, Liaoning, China

Section 1. Characterization of GO

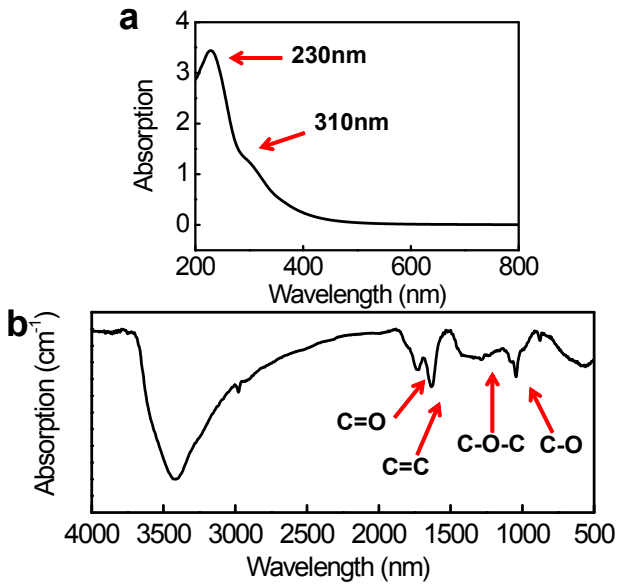

Fig S1. a. Ultraviolet-visible spectrum of GO, the sample has strong absorption at 230 nm, a characteristic shoulder peak at 310 nm.[1] b. Infrared spectrum of GO. Absorption peaks at 1728 cm^{-1}, 1622 cm^{-1}, 1224 cm^{-1} and 1054cm^{-1} represent C=O, C=C, C-O-C and C-O respectively.[2]

Section 2. The analysis of XPS

Through the following equations, we can roughly estimate the content of hydroxyl and epoxide.[3]

$P_{GO} \approx 2P_{epoxide} + P_{hydroxyl} + P_{C=O}$

$P_{oxygen} \approx P_{epoxide} + P_{hydroxyl} + P_{C=O}$

P_{oxygen} is obtained from the O1*s*/C1*s* intensity ratio of GO. P_{GO} is obtained from the C-O and the C=O peaks area to the total C1*s* spectral area. $P_{C=O}$ is obtained from the ratio of C=O peak to the total C1*s* spectral area.

By substituting P_{GO}, P_{oxygen} and $P_{C=O}$ into the equations, the equations can be solved. After photoreduction, $P_{epoxide}$ decreased from 15.8% to 4.1%. At the same time, the $P_{hydroxyl}$ increased from 15.3% to 19.6%.

Section 3 Standard mass spectrum of overall gas products

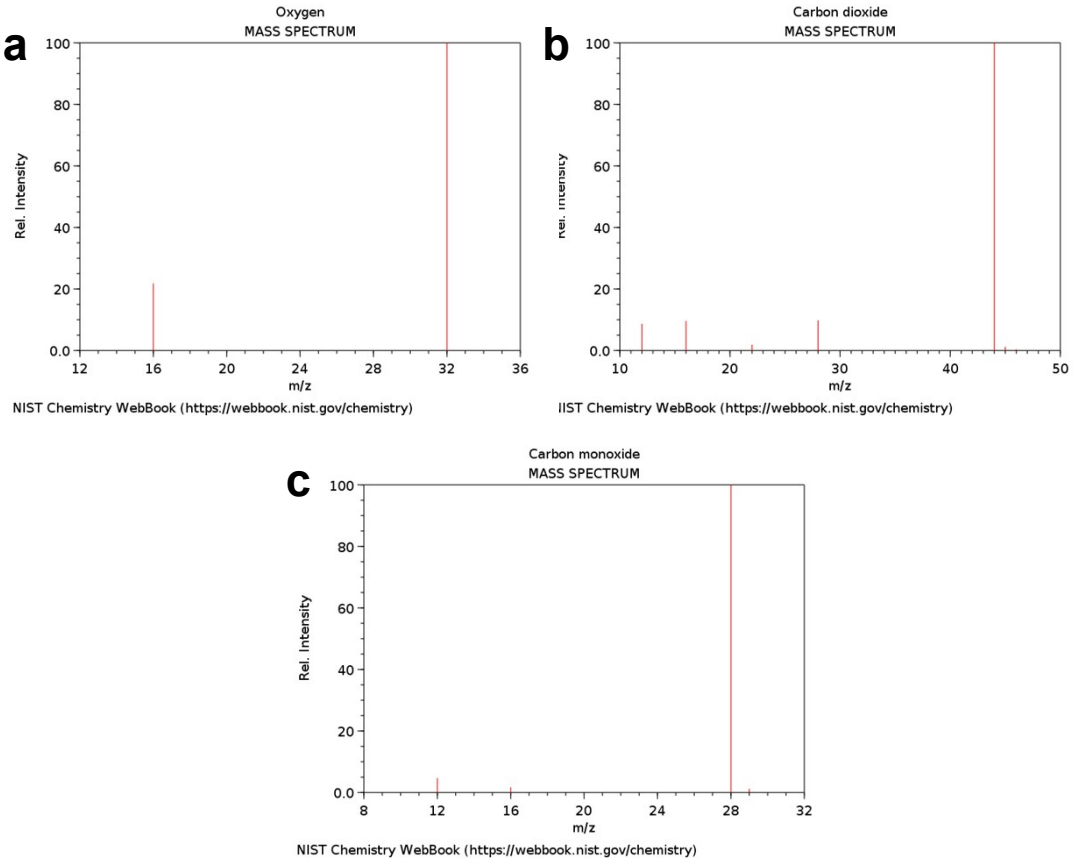

Fig S2. (a) Standard mass spectrum of O_2, (b) Standard mass spectrum of CO_2 and (c) Standard mass spectrum of CO from the NIST database.

Molecular ion peak of O_2, CO_2 and CO are m/z=32 44 and 28, respectively. Therefore, according to the charge-mass ratio of overall gas products provided in Fig S2, we assign m/z=32, 34 and 36 to $^{16}O_2$, $^{16}O^{18}O$ and $^{18}O_2$ in Fig. 3; m/z=44, 46, and 48 to $^{16}CO_2$, $C^{16}O^{18}O$ and $C^{18}O_2$ in Fig. 5, respectively.

Section 4. Mass spectrum of overall gas products

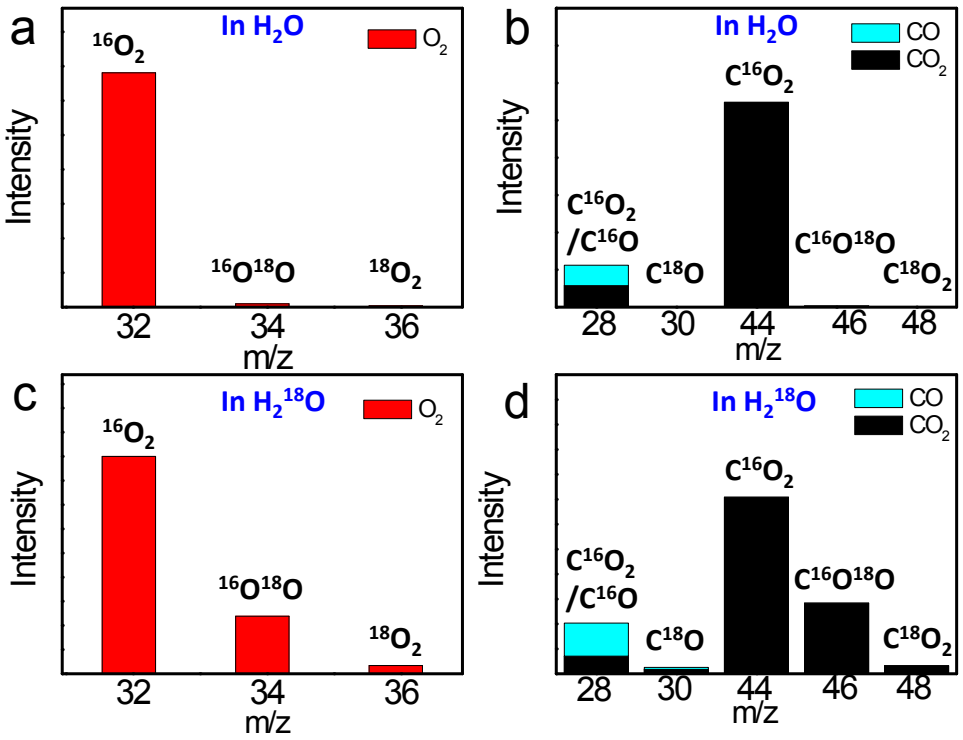

Fig S3. Mass spectrometry signals of overall gas products in normal H_2O (a, b) and in $H_2{}^{18}O$ (c,d), respectively.

m/z=32,34 and 36 are signals of $^{16}O_2$, $^{16}O^{18}O$ and $^{18}O_2$, respectively. m/z= 44, 46, and 48 are signals of $^{16}CO_2$, $C^{16}O^{18}O$ and $C^{18}O_2$, respectively. The ratio of m/z=44 to m/z =28 is higher than the ratio determined by the standard mass spectrometry of CO_2 (Fig S2). Therefore, m/z=28 is assigned to fragmentation peaks of CO_2 and molecular ion peaks of CO, in other words, CO generated in this experiment. In unlabeled experiment, CO may be produced by carbonyl removal. In the labeling experiment, $C^{18}O$ generated accounted for 3% of the total CO, which was in the range of experimental errors (the relative error of mass spectrometry is 3%). Furthermore, this ratio is comparable to the ratio of $^{18}O_2$ in O_2 (2.7%) obtained by the oxygen exchange between GO and $H_2{}^{18}O$. Therefore, $C^{18}O$ has nothing to do with water oxidation.

Section 5. The credibility of the isotope labeled data

In order to prove the repeatability of our experiment, we repeated the labeling experiment with 16% (atom %) ^{18}O water. The results were compared with 20% (atom %) ^{18}O water shown in the following table.

With the decrease of ^{18}O content in water, the proportion of ^{18}O in the generated oxygen decreases correspondingly. The proportion of ^{18}O in produced oxygen is consistent with the mechanism we proposed.

Table S1. Content of different components in isotope labeling experiment

Content of ^{18}O in water (atom %)	The proportion of different oxygen (%)			The proportion of different carbon dioxide (%)		
	$^{16}O_2$	$^{16}O^{18}O$	$^{18}O_2$	$C^{16}O_2$	$C^{16}O^{18}O$	$C^{18}O_2$
20	78.9	18.7	2.4	76.2	22.6	1.2
16	84.2	13.9	1.9	85.2	13.9	0.9

Section 6. The probability calculation of reaction between epoxy/carbonyl and water molecule.

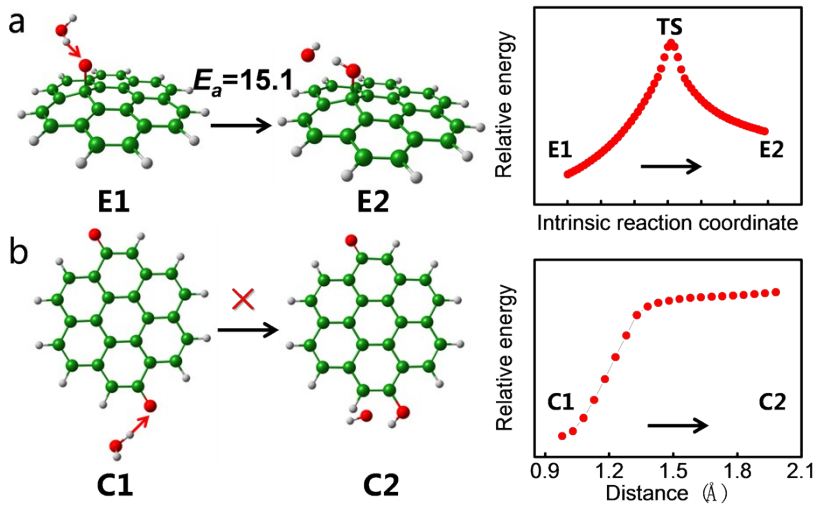

Fig S4. a. The structures of reaction and IRC calculation of H in water molecule transfer to epoxy group, the unit of E_a is Kcal/mol. b. The energy curve obtained by stretching the O-H bond in the water molecule, X axis is the distance between O and H

From the simulation results, H in water molecule can transfer to epoxy group to form hydroxyl group, and the reaction activation energy is 15.1 kcal/mol. We did not find the transition state of H in water transfer to carbonyl in GO. By scanning the energy curve as the O-H bond stretching. We find that as the O-H bond stretching, the energy keeps increasing. Therefore, carbonyl is difficult to react with water molecules from the perspective of energy prediction.

Section 7. Infrared spectrum and Raman spectrum of GO

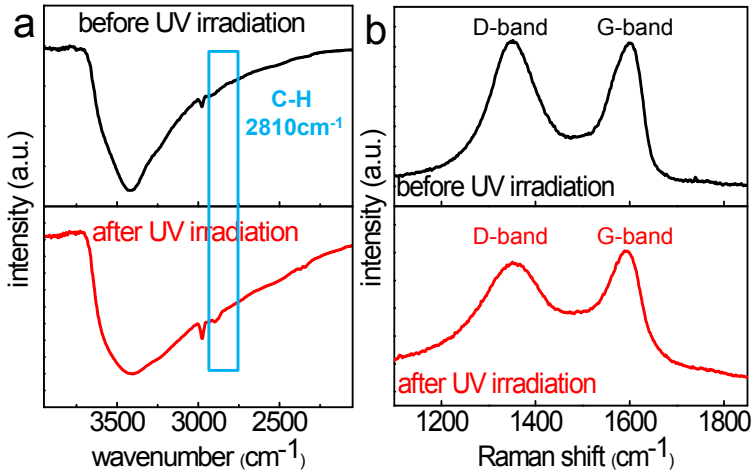

Fig S5. a.Infrared spectrum of GO before and after irradiation. The blue box represents C-H bond absorption.（～2810-2830 cm^{-1}）The C-H bond content has an increasing tendency after illumination, this is support the mechanism we proposed.[3] b. Raman spectrum of GO, before irradiation D band and G band in 1351 cm^{-1}, 1604 cm^{-1} respectively. The ratio of the intensities of the D and G bands I_D/I_G = 1.41. After irradiation D band and G band in 1356 cm^{-1}, 1600 cm^{-1} respectively. The ratio of the intensities of the D and G bands I_D/I_G = 1.32.

Section 8. The effect of water on the generation of CO_2

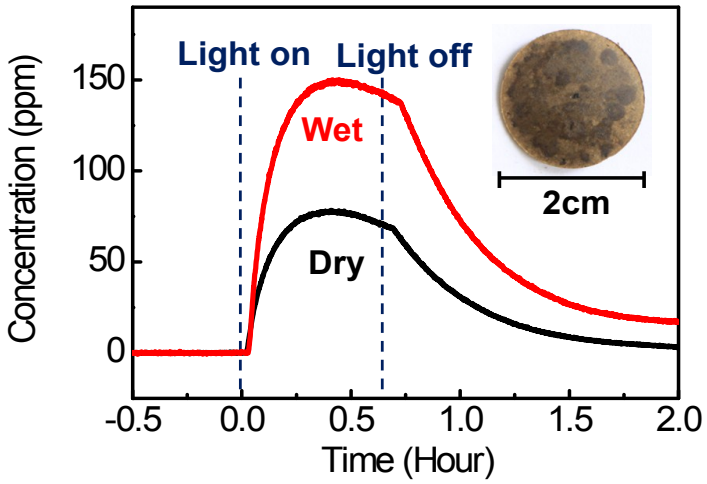

Fig S6. CO_2 signal under UV irradiation in solid sample with low water content and aqueous dispersion sample state obtained by on-line mass spectrum. Insert: photograph of GO tablet we prepared by 50mg GO powder.

Section 9. The concentration changing of O_2 and CO_2 with irradiation time.

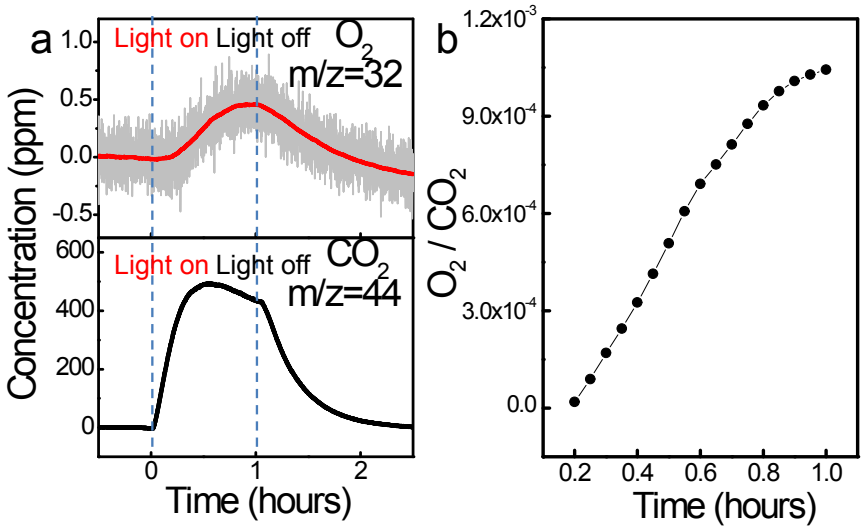

Fig S7. a The concentration of O_2 and CO_2 increased after irradiation, the maximum concentration of O_2 is about 0.5 ppm, the maximum concentration of CO_2 is about 500 ppm. The two signals gradually decreased when the lights were turned off. b. The concentration ratio of O_2 and CO_2 changing with time. The plotting method is to take concentration ratio of O_2 and CO_2 every five minutes from 20 minutes to 60 minutes of Figure a.

If O_2 and CO_2 are produced simultaneously in a definite process, their ratio should be a constant and then the curve of their concentration ratio should be nearly a straight line parallel to the X axis during the whole process of photoreduction. This is inconsistent with our experimental results. In our experiments, the concentration ratio of O_2 and CO_2 is nonlinear relation with irradiation time, which indicates there is no correlation between the formation of O_2 and CO_2, their formation mechanism should be independent.

Section 10. Reaction path of CO_2 evolution reaction

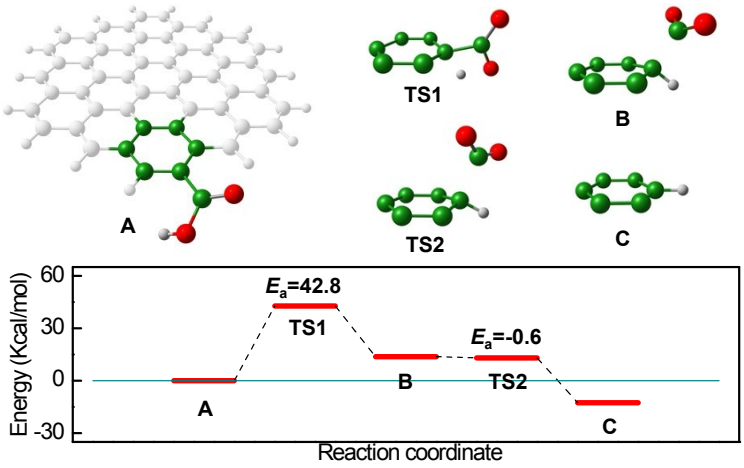

Fig S8. Minimum energy path for decarboxylation obtains by DFT calculation. Configurations of stable state and transition state are shown in the figure. We also omitted the gray part of A. The reaction energy curve including activation energy of the whole reaction is given in the bottom diagram.

Decarboxylation is an appropriate mechanism for CO_2 formation.[4,5] We simulated the reaction pathway of carboxyl removal based on the triplet state by DFT calculation. As shown in Fig S6, the reaction involves two steps. First, the hydrogen atom on the carboxyl group is transferred to the carbon atom adjacent to the carboxyl group. In the second step, the carboxyl groups without a hydrogen atom are directly removed to produce CO_2. The activation energy of the reaction process demonstrated that the first step is the rate-determining step of the whole reaction (Figure S6 and Scheme S2).

However, the XPS analysis results indicated that the carboxyl is reduced only from 15.7% to 12.1% after photoreduction. But the amount of CO_2 is much larger than that of O_2. This phenomenon can be explained if we considered that the epoxy and carbonyl groups in GO may be converted into carboxyl groups in the process of photoreaction. Additionally, we proved our conjecture using the DFT approach. According to the results, the epoxy pair and the carbonyl pair

are distributed at the edge of the GO. The XPS analysis cannot clearly distinguish between the epoxy pair and carbonyl pair due to their similar chemical environment. They both can cut GO from the edge like a "zipper".[6,7] We chose the epoxy pair and carbonyl pair as the initial structure of the reaction, separately, as shown in Figure S7. From the value of the activation energy, the epoxy pair is more likely to break the C-C bond. The structure containing the broken C-C bond could continue to react with water molecules to produce carboxyl, as the activation energy of this reaction is only 14 Kcal/mol. In the generated of carboxyl, one oxygen atom comes from the epoxy or carbonyl pairs, and the other one comes from water. This result is in agreement with the isotope labeling experiment result.

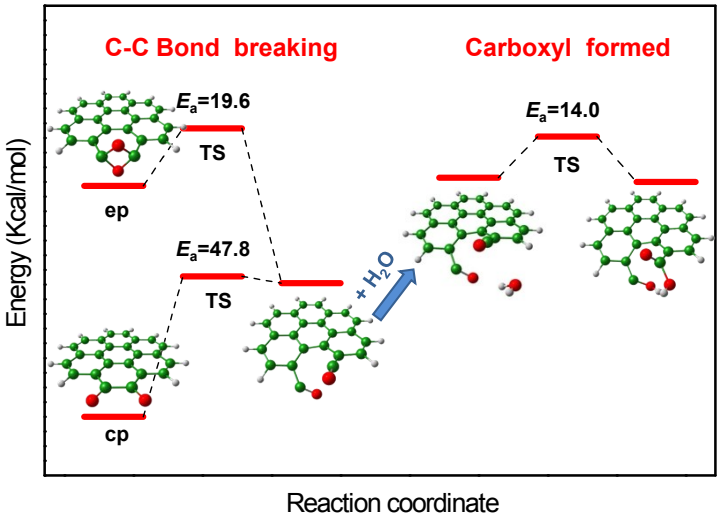

Fig S9. The reaction path and activation energy of epoxy pair (ep) and carbonyl pair (cp) on the edge of GO sheet converted into carboxyl by DFT calculation.

Section 11. Modeling

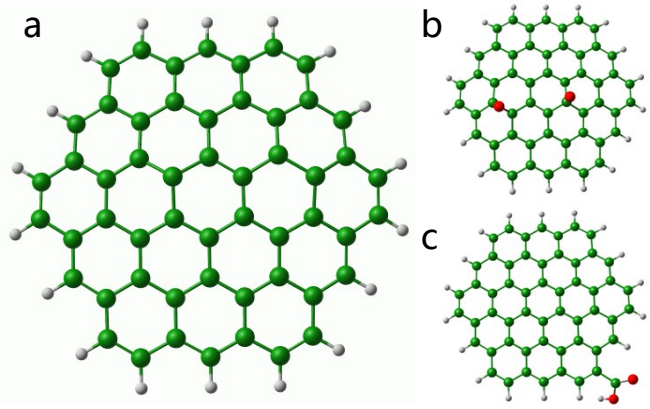

Fig S10. a. The graphene sheets model we selected in calculation. b. The model for oxygen evolution reaction calculation. c. The model for decarboxylation calculation.

The model of graphene sheet contains 54 carbon atoms and 18 hydrogen atoms.[4] The model for oxygen evolution reaction calculation (b in figure S4) contains two epoxy groups in graphene sheet. The model for decarboxylation calculation(c in figure S4) contains one carboxyl at the edge of graphene sheet.

Section 12. The photophysical and photochemical processes of water oxidation.

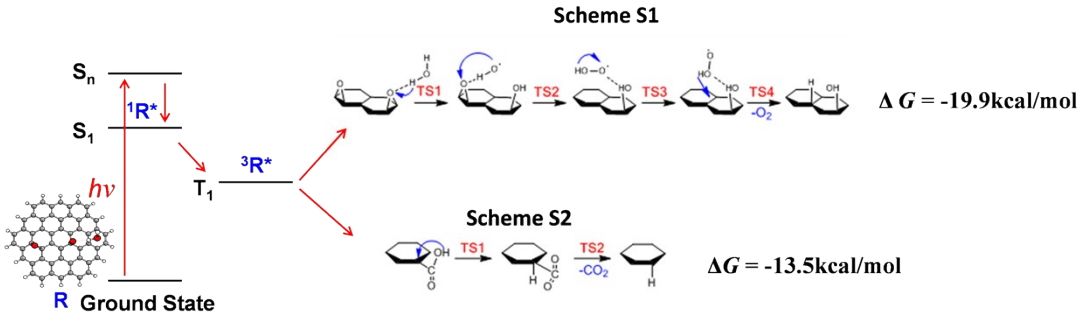

Fig S11. The photophysical and photochemical processes of water oxidation reaction.

The photophysical and photochemical processes of water oxidation reaction are as follows: GO (R) is excited to the S1 state ($^1R^*$) by absorbing photon (*hv*), then transfers to the T1 state ($^3R^*$) through the intersystem crossing and occurs the photochemical reactions. Moreover, we calculated the reaction paths (Scheme S1 and Scheme S2) of water oxidation reaction under T1 state. Scheme S1 is the mechanism of oxygen evolution reaction. Scheme S2 is the mechanism of decarboxylation. Gibbs free energies (ΔG) of Scheme S1 and Scheme S2 are -19.9 kcal/mol and -13.5 kcal/mol, respectively.

Section 13. Experimental Procedures

Preparation of GO. Graphene oxide (GO) was purchased from Nanjing XFNANO Materials Tech Co. Ltd. (China). 20% (atom %) heavy oxygen (^{18}O) enriched water was purchased from Jiangsu Huayi Technology Co. Ltd. (China). Ozone was used to treat the sample to increase oxygen-containing groups and the dispersivity of GO in water. With typical ozone pretreatment, 0.08 g GO powder was dis-persed into 20 ml deionized water, then, the suspension was bubbled by ozone (1L/min) for 30 min. Finally, the sample was separated by centrifugation and the precipitate was redispersed by normal water or ^{18}O en-riched water.

Characterizations. The powder samples of GO or rGO used in characterizations were further dried using a freeze dryer. XPS spectra of GO or rGO powder were measured by ESCALAB250 (Thermo VG) X-ray photoelectron spec-trometer. The ssNMR spectra of GO or rGO powder were collected on an Agilent DD2 500 (B0=11.7 T) spectrometer with 4 mm MAS rotors spun at 10 kHz. The resonance fre-quency of 1H MAS NMR spectrum is 499.81MHz. The 1H spectra were referenced to adamantane at 1.93 ppm. UV-vis absorption spectra were recorded on by Lambda 750s UV spectrophotometer. Raman spectra of GO powder were performed on a DXR Microscope spectrometer. Infrared absorption spectra of GO powder were obtained by a Thermo Fisher 6700 spectrometer.

Photoreduction. GO photoreduction were performed with helium atmosphere in a quartz photochemical reactor at 25 ℃. The UV irradiation source was a high-voltage mercury lamp (1000 W). Mass spectrum (MS) was recorded on a GSD301O3 mass spectrometer (Pfeiffer Vacuum Germany). Helium (3.5ml/min) was used as carrier gas. Before MS detecting, the photochemical reactor was purging with helium continually for 2 hours to remove the air. GO photoreduction was started by switching on the UV irradiation. After 3 hours irradiation, we collected the gaseous products and analyzed the result using MS.

Section 14. Calculation Details.

The density functional theory (DFT) calculation was performed by Gaussian09 software pack-age[8] at B3LYP level.[9] All calculations were done in triplet state of ground state to simulate photoreaction. Geometry optimizations, activation energies and frequencies were carried out with the 6-31G (d) basis set.[10,11] All configurations of transition State were confirmed by the analytical calculation of their frequencies. Intrinsic reaction coordinate (IRC) analyze was used to verified all stationary points configurations. Zero-point correction was employed to eliminate the error of activation energy.

Reference

(1) Abdelsayed, V.; Moussa, S.; Hassan, H. M.; Aluri, H. S.; Collinson, M. M.; El-Shall, M. S. *The Journal of Physical Chemistry Letters* **2010**, *1*, 2804.

(2) Krishnamoorthy, K.; Veerapandian, M.; Yun, K.; Kim, S. J. *Carbon* **2013**, *53*, 38.

(3) Kim, S.; Zhou, S.; Hu, Y.; Acik, M.; Chabal, Y. J.; Berger, C.; de Heer, W.; Bongiorno, A.; Riedo, E. *Nat Mater* **2012**, *11*, 544.

(4) Gao, X.; Jang, J.; Nagase, S. *The Journal of Physical Chemistry C* **2009**, *114*, 832.

(5) Plotnikov, V. G.; Smirnov, V. A.; Alfimov, M. V.; Shul'ga, Y. M. *High Energy Chemistry* **2011**, *45*, 411.

(6) Li, Z.; Zhang, W.; Luo, Y.; Yang, J.; Hou, J. G. *J Am Chem Soc* **2009**, *131*, 6320.

(7) Fujii, S.; Enoki, T. *J Am Chem Soc* **2010**, *132*, 10034.

(8) Frisch, M. J.; Trucks, G. W.; Schlegel, H. B., Scuseria, G. E., Robb, M. A., Cheeseman, J. R., Scalmani, G., Barone, V., Mennucci, B., Petersson, G. A., Nakatsuji, H., Caricato, M., Li, X., Hratchian, H. P., Izmaylov, A. F., Bloino, J., Zheng, G., Sonnenberg, J. L., Hada, M., Ehara, M., Toyota, K., Fukuda, R., Hasegawa, J., Ishida, M., Nakajima, T., Honda, Y., Kitao, O., Nakai, H., Vreven, T., Montgomery, Jr., J. A., Peralta, J. E., Ogliaro, F., Bearpark, M., Heyd, J. J., Brothers, E., Kudin, K. N., Staroverov, V. N., Kobayashi, R., Normand, J., Raghavachari, K., Rendell, A., Burant, J. C. Iyengar, S. S. Tomasi, J. Cossi, M. Rega, Millam, N. J., Klene, M. Knox, J. E., Cross, J. B., Bakken, V., Adamo, C., Jaramillo, J., Gomperts, R. E. Stratmann, O. Yazyev, A. J. Austin, R. Cammi, C. Pomelli, J. W. Ochterski, R. Martin, R. L., Morokuma, K., Zakrzewski, V. G., Voth, G. A., Salvador, P., Dannenberg, J. J., Dapprich, S., Daniels, A. D., Farkas, O., Foresman, J. B., Ortiz, J. V., Cioslowski, J., and Fox, D. J. Gaussian, Inc., Wallingford CT 2009.

(9) Becke, A. D. The *Journal of Chemical Physics* **1993**, 98, 5648.

(10) Hehre, W. J.; Ditchfield, R.; Pople, J. A. *J. Chem. Phys.* **1972**, *56*,2257.

(11) Hariharan, P. C.; Pople, J. A. *Mol. Phys.* **1974**, *27*, 209